ACS Catalysis

RESEARCH ARTICLE

pubs.acs.org/acscatalysis

Influence of Polymorphic ZrO_2 Phases and the Silver Electronic State on the Activity of Ag/ZrO_2 Catalysts in the Hydrogenation of CO_2 to Methanol

R. Grabowski,* J. Słoczyński, M. Śliwa, D. Mucha, and R. P. Socha

Institute of Catalysis and Surface Chemistry, Polish Academy of Sciences, ul. Niezapominajek 8, 30-239 Kraków, Poland

M. Lachowska and J. Skrzypek

Institute of Chemical Engineering, Polish Academy of Sciences, ul. Bałtycka 5, 44-100 Gliwice, Poland

Supporting Information

ABSTRACT: Ag/ZrO_2 and $Ag/ZrO_2/ZnO$ catalysts obtained by the coprecipitation method were studied in the CO_2 hydrogenation to methanol. The catalyst structure was determined using X-ray diffraction (XRD) and Thermo-Programmed Reduction (TPR). The X-ray Photoelectron Spectroscopy (XPS) and Auger spectroscopies were used to determine the silver electronic state. It was found that selection of the appropriate conditions of the catalyst preparation influences silver dispersion degree, its electronic state, and contents of the zirconia polymorphic phases (tetragonal and monoclinic). The presence of oxygen vacancies stabilizes both the thermodynamically unstable t-ZrO_2 phase and the Ag^+ cations, which are present in the vicinity of oxygen vacancies. The catalytic activity to methanol increases with increasing t-ZrO_2 content but RWGS reaction is accelerated by dispersed metallic silver. The implications of the obtained results for the mechanism of the catalytic hydrogenation of CO_2 are discussed.

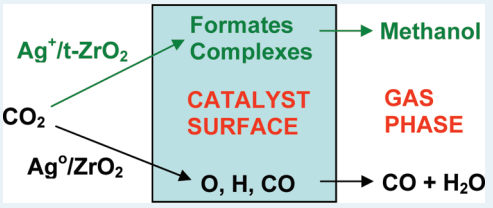

KEYWORDS: CO_2 hydrogenation, methanol synthesis, silver zirconia catalysts

1. INTRODUCTION

Synthesis of methanol from CO_2 has been widely studied during the past years. Processing cheap raw materials such as CO_2 and the need to mitigate the greenhouse effect have been among the reasons behind this research.[1−3] Another important reason has been the search for new energy sources. The cycle hydrogenation of CO_2−steam reforming of methanol can become a mobile source of hydrogen which is applied in the fuel cells.[4−6]

Systems containing copper and ZrO_2, also in combination with other oxides (ZnO, Al_2O_3, Ga_2O_3, etc.), are active in the reaction of hydrogenation of CO_2 to methanol.[7−22] Alternative catalysts, containing silver in the place of copper, are less active in the methanol synthesis and for that reason they have been less investigated.[23−27]

The data concerning the selectivities of these catalysts are not entirely univocal. Baiker et al.[23] and Köppel et al.[25] think that selectivities to methanol in hydrogenation of CO_2 for both Ag/ZrO_2 and Cu/ZrO_2 catalysts are similar. However, closer analysis of the results included in the paper,[25] shows that in comparison with Cu/ZrO_2 catalyst the silver catalyst has a little higher selectivity at lower temperature (below 500 K). However, closer analysis of the results included in the paper,[25] reveals that silver catalyst exhibits slightly higher selectivity to methanol at lower temperature (below 500 K) in comparison with Cu/ZrO_2 catalyst. Moreover, Fröhlich et al.[24] pointed out that doping of Cu/ZrO_2 with silver leads to the increase of the selectivity to methanol without change of CO_2 conversion. According to the paper of Rhodes and Bell,[28] for the Cu/t-ZrO_2 catalyst, at the conversion below 1%, methanol selectivity is in the range 75−95% and depends on the reaction temperature and the catalyst preparation, while the selectivity to methanol for silver catalysts obtained in the same conditions is around 100%.

Structure and operational mechanism of the copper catalysts have been extensively studied. A synergy between active metal and ZrO_2 or ZnO was found in these systems, and it is believed that the stabilization of Cu^+ ions on the surface of the catalyst plays an important role in this phenomenon.[24,29−36] The presence of Cu^+ facilitates the adsorption of CO_2 and the formation of the transitive complexes leading to the formation of methanol.[29,30,34−37] It is widely accepted that the hydrogenation of the formate type complexes is the rate determining step of the reaction.[37,38] On the other hand, the parallel RWGS process occurs in accordance with the simple redox mechanism on the surface of metallic Cu.[37−41] In contrast, no systematic information on the mechanism of hydrogenation of CO_2 to methanol over silver containing catalysts has been available.

The aim of this paper is to find out if the synergy effect, analogous to that postulated for the copper catalysts, exists in the

Received: October 5, 2010
Revised: January 10, 2011
Published: February 24, 2011

Ag/ZrO_2 and $Ag/ZrO_2/ZnO$ systems and to elucidate the mechanism of such synergy. Structural modifications in the Ag/ZrO_2 and $Ag/ZrO_2/ZnO$ systems were introduced by changing the composition and preparation methods, and these modifications were correlated with the activity and selectivity of the catalysts in the hydrogenation of CO_2 to methanol.

2. EXPERIMENTAL SECTION

2.1. Preparation. The oxide precursors of the catalysts were synthesized by the coprecipitation method using NaOH or Na_2CO_3 as the precipitant agent. The solution containing appropriate amounts of $AgNO_3$ and $ZrO(NO)_2$ with a possible addition of $Zn(NO_3)_2$, and the precipitant solution were added simultaneously drop by drop to a vessel containing demineralized water. The precipitation was performed at a constant temperature of about 353 K, constant pH of 7 or 9 for Na_2CO_3 and NaOH, respectively, and under vigorous mixing. After the precipitation, the mother liquid was held at 353 K and under mixing for 1 h. After cooling down the mixture to ambient temperature, the precipitate was separated by 5-fold centrifugation at 3500 rpm and washed with demineralized water. Then, the precipitate was dried at 373 K, milled, and subsequently calcined at 623 K for 10 h in the air flow. After cooling down, the obtained oxide precursor was milled again. The Aldrich reagents of 99.99% purity were used. The molar ratio of ZrO_2 to ZnO in the precursors containing zinc was constant and corresponded to the $3ZnO\text{-}ZrO_2$ stoichiometry. According to Nitta et al.,[42] such composition is optimal for the copper catalysts used in the methanol synthesis from CO_2. Ag_2O was obtained from $AgNO_3$ by the precipitation of AgOH using NaOH solution. $3ZnO\text{-}ZrO_2$ and ZrO_2 supports were obtained using the methodology described for the precursors but without any silver addition. The catalysts' composition was controlled by determination of metallic components (Ag, Zr, and Zn) by ICP-OES method using a Perkin-Elmer spectrometer Optima 2100DV .

2.2. X-ray Diffraction (XRD) Measurements. Diffraction patterns of the oxide precursors and the used catalysts were collected with a Bruker AXS D505 powder diffractometer. CuKα radiation and a graphite monochromator of the secondary beam were used. The quantitative phase contents and the crystallite sizes of the catalyst components were estimated by a multiphase Rietveld refinement using the TOPAS software. The fundamental parameter calculations were carried out according to ref 43.

2.3. Electron Spectroscopy. The X-ray Photoelectron Spectroscopy (XPS) and X-ray Auger Electron Spectroscopy (XAES) measurements were performed in an ultrahigh vacuum (3×10^{-10} mbar) system equipped with a hemispherical analyzer (SES R 4000, Gammadata Scienta). The unmonochromatized MgKα source of incident energy of 1253.6 eV was applied to generate the core excitation. The spectrometer was calibrated according to ISO 15472:2001. The energy resolution of the system, measured as a full width at half-maximum (fwhm) for the Ag $3d_{5/2}$ excitation line was 0.9 eV.

For the analysis, powder samples were pressed into indium foil. The analysis area of thus prepared samples was about 3 mm^2. No gas release and no change in the sample composition were observed during the measurements.

The CasaXPS 2.3.12 program was applied for the analysis of the XPS and XAES spectra. The spectra were calibrated using the maximum of the C 1s core excitation at the electron binding energy (BE) of 285 eV (this peak can be assigned to the adsorbed hydrocarbons treated as an internal standard). In the spectra, the background was approximated by a Shirley profile. The spectra deconvolution into a minimum number of the components was done by application of the Voigt-type line shapes (70:30 Gian/Lorentzian product).

2.4. Scanning Electron Microscope Measurements. The study of the morphology and chemical composition of the silver catalysts were carried out by means of JEOL JSM-7500F Field Emission Scanning Electron Microscope with the EDS (energy dispersive spectra) detection system of characteristic X-ray radiation. K575X Turbo Sputter Coater was used for coating the catalysts with chromium (deposited film thickness, 20 nm).

2.5. Thermo-Programmed Reduction (TPR). The reducibility profiles of the oxide precursors and their components were obtained using a u-shape quartz flow reactor (diameter ca. 5 mm). About 0.3 g of the precursors or 0.1 g of each given component was mixed with about 0.25 g of Al_2O_3. A 0.1 g portion of the mixture was used for the TPR measurements. A mixture of 5% H_2 in Ar was used as a reducing agent. Before the TPR analysis, all the samples were kept in a stream of helium at 373 K for 1.5 h to remove physically adsorbed water. Subsequently, each sample was cooled down to ambient temperature, and the TPR analysis was performed with a temperature ramp of 10 deg/min and a flow rate of the reducing mixture of 30 cm^3/min. The water formed during the reduction was removed by a cold trap. The TPR profiles were recorded using a TCD detector.

2.6. Catalytic Measurements. The activity of the catalysts was tested in a high pressure fixed bed flow stainless steel reactor (vol. ca. 8 cm^3) connected online to a gas chromatograph, equipped with a TCD detector (analysis of H_2, CO, and CO_2) and a FID detector (organic compounds). All lines were heated to 393 K to prevent condensation of methanol and water. Reactor internal diameter was 8 mm; a thermocouple was placed in the middle of the catalyst layer which was put between two layers of the porcelain of the same grain size as catalyst. One cm^3 of a catalyst with the grain size 0.64−1 mm was placed into the reactor. The oxide precursors were reduced in a stream of diluted hydrogen (5 vol % H_2 in N_2) at 473 K under atmospheric pressure for 3 h and activated in the mixture of reactants by raising the temperature by steps of 30 deg between 473 and 623 K every 2 h. The catalytic activity in the methanol synthesis was determined under the following conditions: pressure 8 MPa, temperature range 453−533 K, space velocity of the reactants flow GHSV = 3600 h^{-1}, composition of the reactant mixture $H_2/CO_2 = 3$. It was checked in the preliminary experiments, in which mass and grain size of the catalysts were varied and temperature profile was determined, that under these conditions mass and heat transfer did not limit the reaction rate. After the reduction and activation, the catalysts showed a constant activity for 10 days in the cycles of the temperature increase and decrease. After the tests, the catalysts were cooled down to room temperature in the reaction mixture. Such catalysts are named in this paper as "used catalysts". It is assumed that the composition and structure of the used catalysts correspond closely to the composition and structure of the working catalysts at the stationary state which is established under conditions of the catalytic reaction.

3. RESULTS

3.1. Phase Composition and Morphology of the Catalysts. Symbols, nominal compositions of the studied catalysts, and specific surface areas of the oxide precursors are listed in Table 1.

dx.doi.org/10.1021/cs100033v |ACS Catal. 2011, 1, 266–278

Table 1. Characterization of the Silver Catalysts

		nominal composition [at %]			
precipitant	symbol	Ag	Zr	Zn	surface area [m^2/g] precursor/used catalyst
NaOH (pH = 10)	ZrAg10	10	90	0	170/102
	ZrAg30	30	70	0	115/60
	ZrZnAg10	10	22.5	67.5	102/41
	ZrZnAg30	30	17.5	52.5	30/26
	ZnAg10	10	0	90	5/5
Na_2CO_3 (pH = 7)	ZrAg30	30	70	0	58/11
	ZrZnAg10	10	22.5	67.5	41/30
	ZrZnAg30	30	17.5	52.5	44/25
	ZrZnAg62.5	62.5	9.4	28.1	19/15
	ZnAg10	10	0	90	34/21

The results show that the usage of NaOH as the precipitant leads to the formation of precursors with considerable higher specific surface areas in comparison with the analogous precursors obtained by the precipitation with Na_2CO_3. In the NaOH series, the observed decrease in the surface area follows the increase in the Ag and ZnO content. The surface areas of the samples from the Na_2CO_3 series are much more uniform and no correlation with the content of particular phases is observed. In both series, a decrease in the specific surface area of the catalysts takes place during the reaction. These changes cannot be further analyzed because the time on stream and temperature were not always the same for all the catalysts during the measurements.

The XRD patterns of the selected precursors and the used catalysts from both series (NaOH and Na_2CO_3) are shown in Figure 1. The crystallization of ZnO and Ag occurs in the zinc oxide containing precursors. In contrast, the crystallization degree of silver is small or even unnoticeable in the samples with the same Ag content but without ZnO. The presence of ZrO_2 in the precursors is manifested by a broad peak in the range of $2\Theta = 30°$, where the main diffraction maxima characteristic of two phases are located: the thermodynamically stable monoclinic modification (m-ZrO_2) and the tetragonal one (t-ZrO_2) which is unstable at ambient temperature. The Rietveld method was used for the diffraction peaks' deconvolution and the content evaluation of both phases. An example of such deconvolution for two catalysts with different t-ZrO_2/m-ZrO_2 ratios is presented in Figure 2. It can be concluded from the comparison of the XRD patterns shown in Figure 1 panels A, B and C, D that the noticeable crystallization of the metallic silver and both types of ZrO_2 is a result of a long-term treatment of the catalysts in the reactant flow under a condition of high pressure (8 MPa) and at an elevated temperature (473−533 K). Incidentally, the formation of small amounts of $ZnCO_3$ was observed in the case of the ZrZnAg30 catalyst (Na_2CO_3).

The results of full quantitative XRD analysis by the Rietveld method are shown in Table 2, which comprises the quantitative composition of the used catalysts and the comparison between crystal sizes of the equivalent phases in the precursors and the used catalysts. In the same table the results of chemical analysis of chosen catalysts are presented. As can be seen, the contents of particular phases are close to their nominal values. The discrepancies are in the limit of an error of the implemented method. The comparison of both series of catalysts at the stationary state reveals that the t-ZrO_2 phase content in the NaOH series is considerably higher than in the corresponding catalysts in the Na_2CO_3 series. Furthermore, the catalysts of the NaOH series exhibit a relatively high dispersion of Ag, particularly in samples containing only ZrO_2. In the Na_2CO_3 series, the Ag crystal sizes are significantly higher, and the addition of ZnO favors the silver aggregation. The crystal sizes of ZnO are similar in both series and independent of the catalyst compositions. Both polymorphic phases of zirconium oxide are microcrystalline. In the Table 3 the lattice parameters of the tetragonal ZrO_2 are presented for the catalysts which contain significant amount of this phase. The tetragonal ZrO_2, which is present in the used catalysts, exhibits decreased dimensions of the lattice in comparison with the standard values (PDF-4[44]), which corresponds with partial reduction of ZrO_2 and the formation of oxygen vacancies.[45]

The SEM measurements were carried out to show the metallic silver distribution in the studied catalysts. For example, the SEM imaging of two catalysts, ZrAg10 (NaOH) and ZrAg30 (Na_2CO_3), are presented in Figure 5. As observable from Figure 5 panels A, B, and C, the polydispersive silver crystals (white spots) are deposited on ZrO_2 polycrystalline aggregates. Scanning analysis of the chosen fragment of catalyst surface (Figure 5C) shows that white spots are silver microcrystallites. Much finer crystallites of silver are visible in the electronic version of the images. EDS analysis showed that about 5 to 10% of the surface silver content is finely dispersed and stays in close contact with ZrO_2.

3.2. Surface Properties of the Catalysts. The surface composition of the selected silver catalysts (5) was determined using XPS (Tables 4, 5, and 6). The analytic depth of the method was 6.6 nm in the studied samples.[46] For the ZrAg30(NaOH) samples, the XPS technique gives a Ag/Zr surface ratio in the range of 0.6−0.7, which points to the surface enrichment in silver when compared to the nominal Ag/Zr bulk ratio of 0.43. In ZrAg10(NaOH) sample, the Ag/Zr ratio was equal to the bulk composition (0.1). The silver (Ag^0 and Ag^+) deficiency at the surface was observed in all samples obtained by the Na_2CO_3 method. Moreover, this amount was approximately 50% lower than the one found for the catalysts obtained by the NaOH method. Carbon compounds and small amounts of sodium and phosphorus are the main surface contaminants of all analyzed catalysts.

The C 1s spectra (see the Supporting Information) are dominated by the component assigned to the C−C bonds (BE = 285 eV), but two other components related to C═O bonds (287.5 eV) and to CO_3 (289.6 eV) are also observed. The presence of these maxima hints to an adsorptive origin of the

dx.doi.org/10.1021/cs100033v |ACS Catal. 2011, 1, 266–278

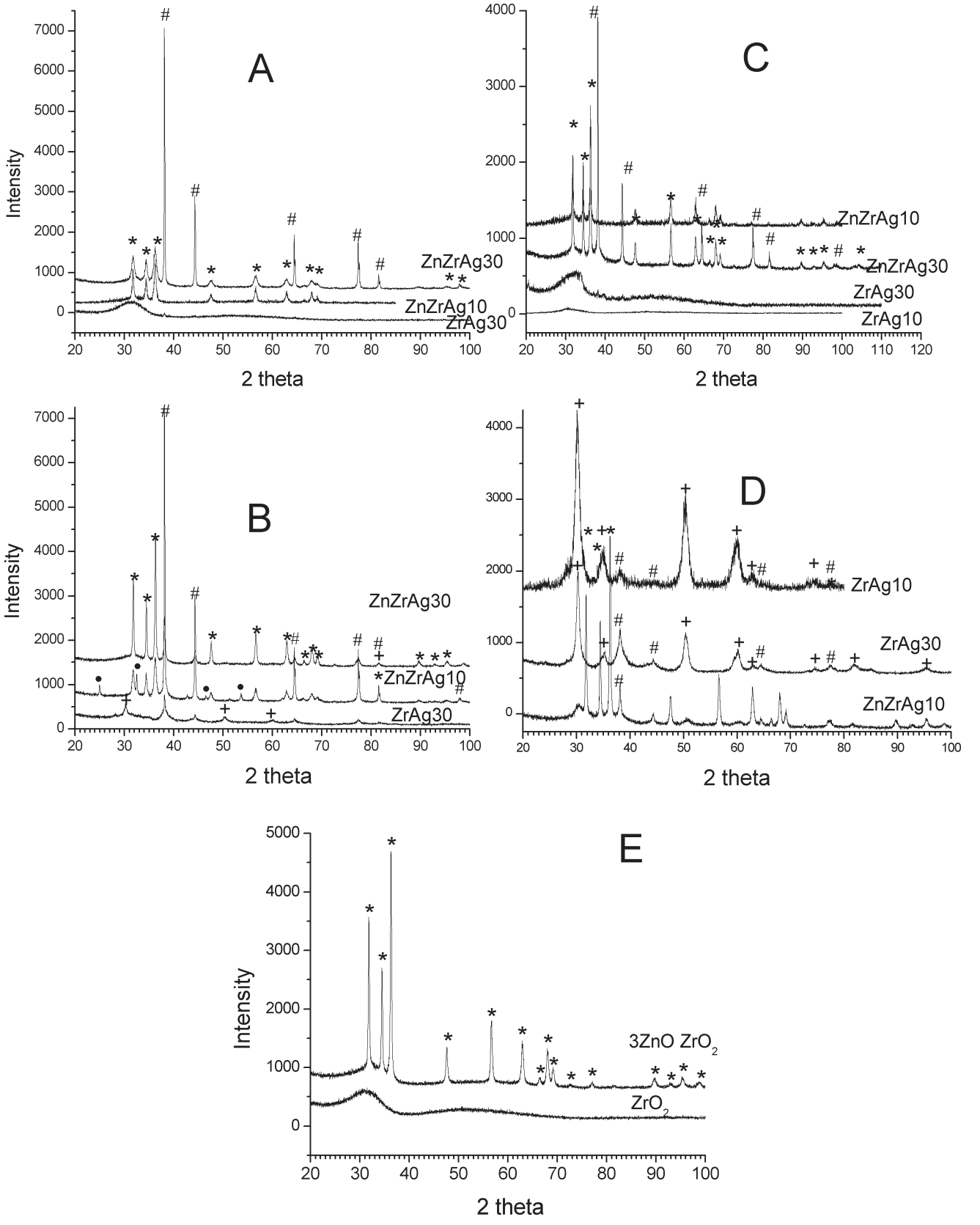

Figure 1. XRD patterns of AgZnZr catalysts obtained by Na_2CO_3 (A, B) and NaOH (C,D) methods: precursors (A, C), used catalysts (B, D), and supports (E). Keys: *, ZnO; #, Ag; +, ZrO_2; ●, $ZnCO_3$.

dx.doi.org/10.1021/cs100033v |*ACS Catal.* 2011, 1, 266–278

carbon impurities (adsorption of hydrocarbons and CO_2 from the ambient environment). Only in case of the sample obtained by the Na_2CO_3 method is the C 1s peak assigned to carbonates showed larger intensity, that is, 34% when compared to the one (around 20%) in the samples obtained by the NaOH method.

The main component in the oxygen O 1s spectra (see the Supporting Information) at BE = 530 eV (65%) is characteristic of the O-metal bond, whereas the peak at 531.8 eV can be assigned to OH groups at the surface. A very limited difference between the concentration of hydroxyl groups in the precursor and in the used catalyst was observed. No significant changes were observed in the Zr 3d spectra for all samples. The main Zr 3d spectrum component (97%) at BE of 182.2 eV was assigned to Zr^{4+} ion in ZrO_2.[47,48] The Zr $3d_{5/2}$ low intensity component at 180.2 eV was found to have similar BE like zirconium cations in oxygen deficient zirconia oxide systems.[49,50] Therefore the latter specie can be attributed to Zr^{4+} ions bonded to oxygen vacancies presented at the zirconia surface.[49]

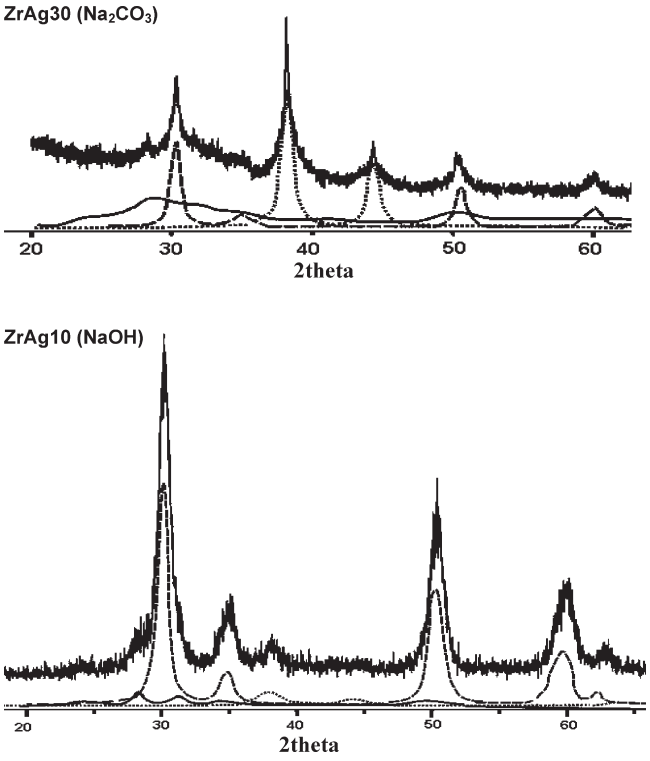

Figure 2. Deconvolution of the XRD patterns for two catalysts, ZrAg30-Na_2CO_3 and ZrAg10-NaOH, with different contents of the tetragonal phase of ZrO_2 (t-ZrO_2). Keys: dashed lines, t-ZrO_2; solid lines, m-ZrO_2; dotted lines, silver.

The Ag 3d spectra of the oxide precursor and the used ZrAg30(NaOH) catalyst were deconvoluted into three components, which are presented in Figure 3 and Tables 5 and 6. An analysis of the small intensity components (A and C) of the Ag 3d core excitation at 366.5 and 369.1 eV (Table 6) points to the presence of Ag^{2+} ions (component A) and Ag nanoparticles/clusters (component C) at the surface of both catalysts. The main spectrum component of above 70% of the overall Ag 3d intensity at BE of 367.9 eV could be assigned to Ag^+ ions.[47,48,51−54] In case of the Ag 3d core excitation, the electronic states of different silver species show limited difference in BE. Therefore, to determine the electronic state of silver in the studied catalysts, the XAES measurements were performed. On the basis of Auger spectra, the modified Auger parameter (α' = Ag $3d_{5/2}$ (BE) + Ag $M_4N_{45}N_{45}$ (KE)) was calculated (Table 5). The analysis of the Auger spectra shape (Figure 4), the values of the Auger parameter and the BE of Ag $3d_{5/2}$ core excitation suggested that silver is present predominantly as Ag^+ ions in all the Ag/ZrO_2 catalysts. Moreover it could be postulated that silver cations are located in an electronegative/electrophilic environment. The claim that the silver cation is surrounded by an electronegative environment was supported mainly by analysis of modified Auger parameters α' and electron binding energies. The BE values obtained for Ag 3d in the studied samples were within the range of parameters presented elsewhere for Ag^+ species.[47,48,51−54] The α' parameter located in the range for metallic silver (slightly above the value for Ag^+ ions) suggested metallic character of the silver species in our samples. However, the shapes of XAES spectra (Figure 4) were similar to the ones

Table 3. Lattice Parameters of Tetragonal ZrO_2

precipitant	catalyst	*a* [Å]	*c* [Å]	*V* [Å^3]
NaOH	ZrAg10	3.605(1)	5.179(2)	67.31(4)
	ZrAg30	3.597(1)	5.167(1)	66.84(2)
	ZrZnAg10	3.58(1)	5.15(1)	66.1(2)
Na_2CO_3	ZrAg30	3.599(2)	5.16(1)	66.8(1)
	PDF-4	3.61(3)	5.21(7)	68(2)

Table 2. Results of Rietveld XRD Analysis for the Silver Catalysts[a]

		composition of used catalysts[wt %] nominal/Rietveld (chemical analysis)					crystallite sizes[nm] precursor/used catalyst			
precipitant	catalyst	Ag	ZnO	$ZrO_{2(m)}$	$ZrO_{2(t)}$	$\Sigma O\rho Z_2$	Ag	ZnO	$ZrO_{2(m)}$	$ZrO_{2(t)}$
NaOH	ZrAg10	9/7	0/0	-/14	-/80	91/94	N/5	-	-/7	-/11
	ZrAg30	27/26	0/0	-/9	-/64	73/73	N/6	-	-/8	-/14
	ZrZnAg10	11/8 (10.8)	59/52 (56.1)	-/0	-/20	30/30 (33.9)	N/20	39/43	-/-	-/N
	ZrZnAg30	34/32 (33.0)	44/68 (46.7)	-/N	-/N	22/N (20.5)	45/44	40/45	-/N	-/N
	ZnAg10	13/10	87/90	0	0	0	106/98	40/44	-	-
Na_2CO_3	ZrAg30	27/31 (25.0)	0/0 (0.0)	-/59	-/10	73/69 (74.2)	N/14	-	-/2	-/12
	ZrZnAg10	11/8	59/69	-/21	-/2	30/23	N/32	25/24	-/5	-/9
	ZrZnAg30	34/30 (30.5)	44/46 (50.3)	-/15	-/8	22/23 (19.1)	22/30	61/46/	-/15	-/8
	ZrZnAg62.5	66/71	23/21	-/5	-/3	11/8	-/41	-/45	-/5	-/-
	ZnAg10	13/9	87/91	0	0	0	138/119	19/31	-	-

[a] N, indeterminable; "-", lack of data.

dx.doi.org/10.1021/cs100033v |ACS Catal. 2011, 1, 266–278

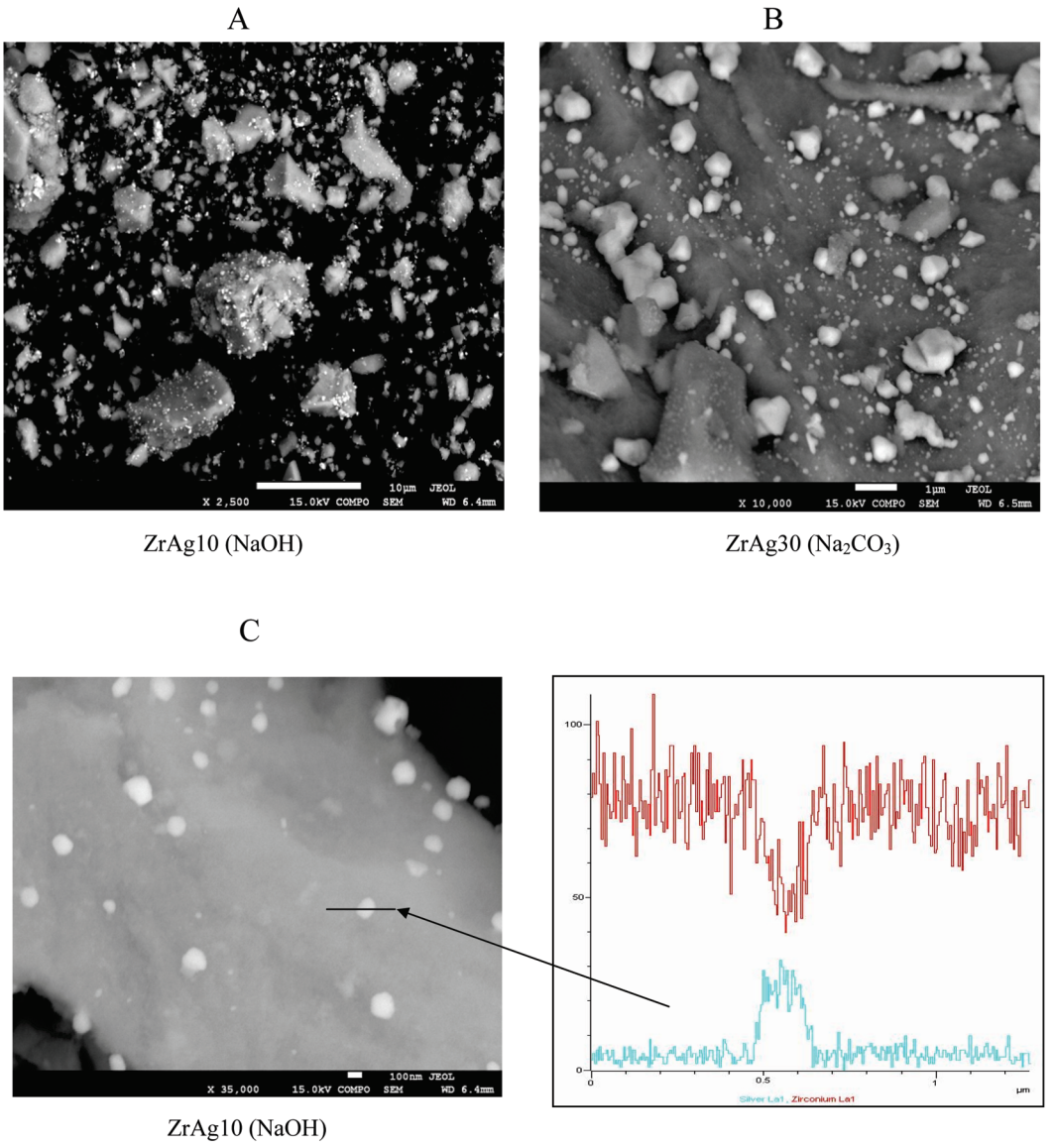

Figure 5. SEM imaging of silver catalysts. (A) ZrAg10 catalysts obtained by NaOH method; (B) ZrAg30 catalysts obtained by Na_2CO_3 method; (C) scanning analysis of chosen silver crystal (~100 nm).

Table 4. Surface Composition of AgZr30 (NaOH) Catalyst

	surface composition (at %)					
sample	O	C	Ag	Zr	Na	P
Oxide precursor	46.4	17.3	14.2	21.0	0.8	0.3
Used catalyst	44.7	16.1	14.3	23.6	1.1	0.1

observed in $AgNO_2$ and Ag_2O with relatively large $M_4V_5V_5$ excitation at KE of 350 eV.[51] Moreover, all other samples obtained with either NaOH or Na_2CO_3 method after the reaction showed the maximum of Ag 3d excitation at BE in the range of 367.2−367.9 eV, that is, in the range observed for Ag^+ species.[47,48] Additionally in the latter case, the α′ parameter showed the values in high range of metallic silver whereas the shape of Auger spectra was similar to the one for Ag^+ in $AgNO_2$ and Ag_2O. Therefore, the electronic state of silver seems to be similar to that in $AgNO_2$ that can be assigned to Ag^+ in an electronegative environment. This leads to the conclusion that Ag^+ can be located in the vicinity of the oxygen vacancies of ZrO_2. The ZrAg30 catalysts obtained using NaOH or Na_2CO_3 differ significantly in the content of the ZrO_2 polymorphic forms. In the NaOH series, the tetragonal form of ZrO_2 is predominating, whereas in the Na_2CO_3 series, a higher content of the monoclinic form is observed (see paragraph 3.1). According to the aforementioned papers,[51−54] a decrease of the α′ parameter reflects an increase in the amount of Ag^+ at the expense of the metallic silver. Guided by this rule one can state that the oxidation degree is higher in the precursor in comparison to the used catalysts. It seems that the presence of the tetragonal phase of ZrO_2 is stabilized by Ag^+ ions connected with oxygen vacancies in the surface layer of the used catalyst.

It is worth noticing that in all ZrAg(NaOH) systems around 80% of silver is at a +1 oxidation state, and no one sample showed silver deficiency at the surface. On the other hand, both analyzed samples that were obtained by the Na_2CO_3 method exhibited silver deficiency at the surface. Moreover, the sample containing zinc (ZnZrA10) showed relatively low amount of Ag^+ ions.

dx.doi.org/10.1021/cs100033v |ACS Catal. 2011, 1, 266–278

Table 5. XPS and XAES Data for the Studied Catalysts

sample	Ag MVV [KE] (eV)	Ag $3d_{5/2}$ [BE] (eV)	α′ (eV)	Ag/Zr	Ag^+/Zr
oxide precursor ZrAg30(NaOH)	357.5	368.2	725.7	0.68	0.49
used catalyst ZrAg30(NaOH)	358.1	367.9	726.0	0.60	0.48
used catalyst ZrAg10(NaOH)	358.5	367.8	726.3	0.10	0.08
used catalyst ZrAg30(Na_2CO_3)	358.4	367.9	726.3	0.24	0.19
used catalyst ZnZrAg10(Na_2CO_3)	358.4	367.2	725.6	0.17	0.10

Table 6. Components of $Ag3d_{5/2}$ Core Excitations of ZrAg30 Catalysts

	oxide precursor ZrAg30(NaOH)		used catalyst ZrAg30(NaOH)		
component	BE(eV)	%	BE(eV)	%	assignment
A	366.8	19.4	366.8	10.8	Ag2+
B	368.2	72.4	367.9	78.7	Ag+
C	369.3	8.2	368.9	10.5	Ag^0(nano)

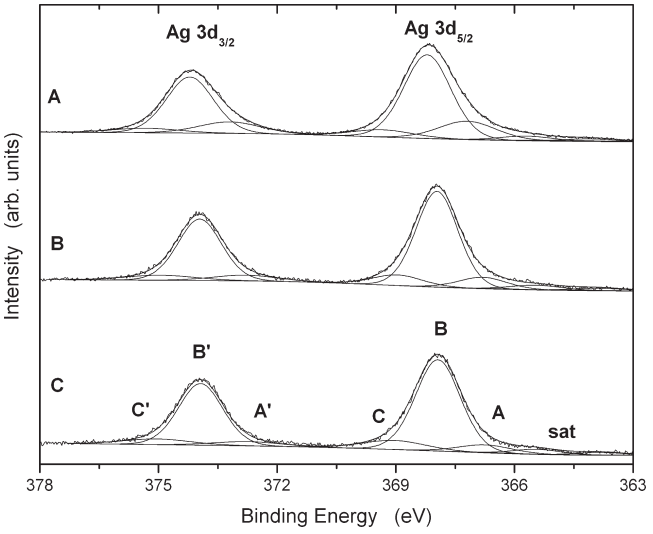

Figure 3. Ag 3d core excitation spectra for ZrAg30 catalysts. (A) Precursor obtained by NaOH method; (B) used catalyst obtained by NaOH method; (C) used catalyst obtained by Na_2CO_3 method.

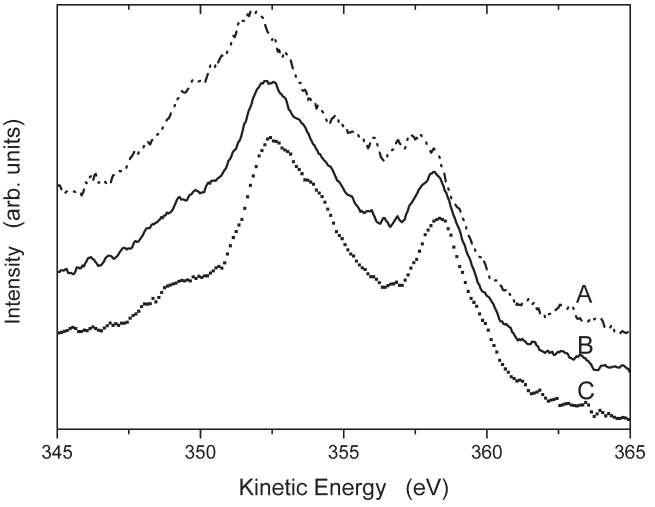

Figure 4. Auger spectra for the ZrAg30 catalysts. (A) Precursor obtained by the NaOH method; (B) used catalyst obtained by the NaOH method; (C) used catalyst obtained by the Na_2CO_3 method.

3.3. Reducibility of the Catalysts. TPR profiles of selected oxide precursors, their components and used catalysts are presented in Figure 6. Silver oxide Ag_2O is reduced quantitatively to metallic silver in the temperature range of 370−450 K (T_{max} = 430 K). Zirconium and zinc oxide undergo a slight reduction, beginning at temperatures of 700 and 800 K, respectively (T_{max} = 740 and 920 K), which is not accompanied by any phase transition. Thus, it can be assumed that the reduction is connected to the formation of oxygen vacancies. Formation of such structural defects is well documented for both oxides.[45]

Characteristic peaks of the components can be found in the TPR profiles of oxide precursors. The reduction of Ag_2O in the precursors is similar to the reduction of the pure phase but is evidently a two-stage process, which points to interactions between Ag_2O and ZrO_2. The TPR maxima of ZrO_2 stay unaltered or shift slightly to higher temperatures, and the presence of silver does not influence considerably the ZrO_2 reduction degree. Calculating the area under the reduction peak, the reduction degree of ZrO_2 in the pure phase and in the precursors can be estimated at 0.5% in relation to the total amount of oxygen in ZrO_2. TPR measurements showed that the reduction of ZrO_2 occurs at higher temperature in comparison with the temperature of reduction and activation of the catalysts in the feed mixture. However, the TPR experiments were performed in dynamic conditions under a low partial pressure of hydrogen (ca. 0.005 MPa). Long treatment of the catalysts in highly reducing mixture (H_2 partial pressure ≈6 MPa) led to a reduction of ZrO_2 and to the formation of oxygen vacancies characteristic for the structure of the catalysts in the stationary state. The above conclusion is confirmed by the TPR profiles of the used catalysts in which no maximum, characteristic for reduction of the surface layer of ZrO_2, is observed since this phase is already reduced. However, continuous hydrogen consumption observed above 700 K may indicate the reduction of the deeper layers of ZrO_2 limited by oxygen diffusion through the defected subsurface layer. In the case of the used catalysts, oxygen vacancies previously formed facilitate this process and make it observable.

3.4. Catalytic Activity. Methanol, water, and carbon monoxide were the only products of the CO_2 hydrogenation under

dx.doi.org/10.1021/cs100033v |ACS Catal. 2011, 1, 266–278

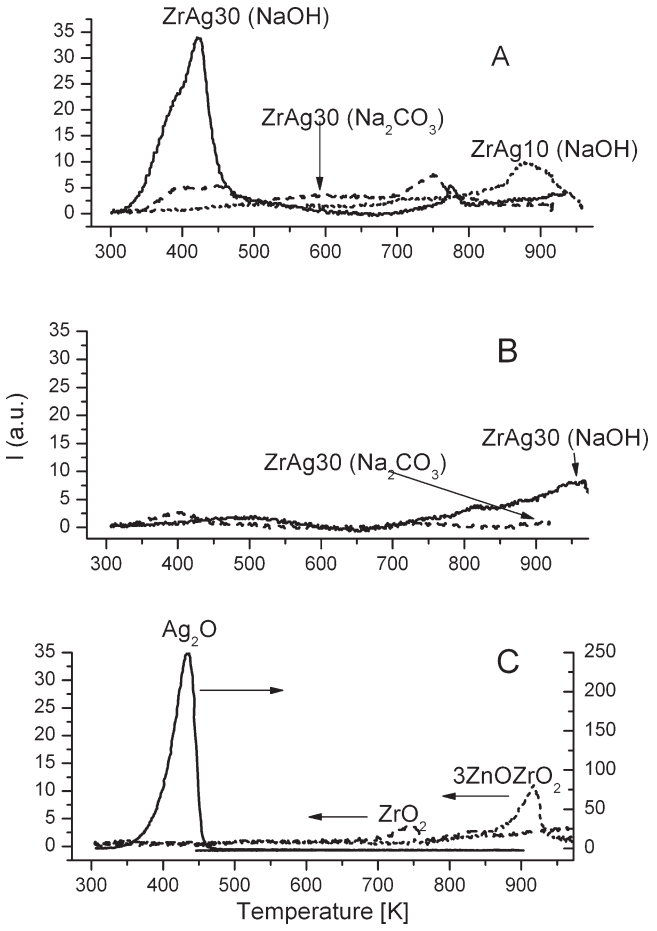

Figure 6. TPR profiles of the selected oxide precursors (A), used catalysts (B), and components of the catalysts (C).

the conditions of the catalytic tests. The observation provides evidence that hydrogenation of CO_2 proceeds according to two parallel reactions.

$$CO_2 + 3H_2 \rightarrow CH_3OH + H_2O \quad (1)$$

$$CO_2 + H_2 \rightarrow CO + H_2O \quad (2)$$

At low conversions and low temperatures, the hydrogenation of CO_2 to methanol is the primary pathway because it is faster than the hydrogenation of CO.[38] In our experiments the total conversion of CO_2 was between 1 and 10% depending on the temperature and the activity of the catalysts. The system is far from equilibrium in such conditions, and the reaction is controlled kinetically. The selectivity to methanol always decreases with increasing temperature, which results from a higher contribution of the endothermic RWGS reaction.

The activity in the CO_2 hydrogenation and the selectivity to methanol for both series of silver catalysts are presented in Figures 7 and 8. The rate of the methanol formation with reference to catalyst mass was taken as a measure of the catalytic activity (space time yield, STY). Such manner of presentation makes for easier searching of the correlation between catalytic activity and catalysts phase composition, as well as selection of the active phase. As observed from Figure 7 and Table 1 the STY of methanol increases proportionally to the specific surface area of the catalysts, which gives evidence that the whole catalyst surface participates in the catalytic reaction and there is the lack of the diffusion limitations.

From Figures 7 and 8 it is visible that the catalysts obtained by using NaOH as the precipitant are more active in comparison with the catalysts obtained by using Na_2CO_3. Among the catalysts from the NaOH series, the activity is connected with the presence of zirconium oxide. The ZnO addition does not influence significantly the methanol space time yield (STY); therefore, the catalysts containing only ZnO and Ag exhibit low catalytic activity. The activation energy determined from plots of temperature versus methanol STY is the same for both series of catalysts and is equal to 45 ± 3 kJ/mol. Thus, the observed differences in the catalytic activity are connected to various values of the pre-exponential factor because of different active site concentrations and do not change in the mechanism of the methanol formation reaction. The results for typical copper catalyst obtained by the carbonate method and tested in the same condition are also presented in Figures 7, 8, and 9. Ample comparison of the copper and silver catalysts' activities is given in ref 27.

As can be seen the methanol yield is lower for the most active silver catalysts when compared to the standard copper catalysts. However, the silver catalysts exhibit higher selectivity if one compares the catalysts at low temperature (453−493 K) at similar conversion to methanol (ZrZnCu10 catalyst according ref 27). The decrease in the selectivity to methanol observed with temperature increase is related to a higher contribution of the RWGS reaction. The differences in the catalyst activity for both series of silver catalysts are clearly illustrated in Figure 9, which presents the plot of the selectivity to methanol versus the yield to methanol. The relationships obtained for both NaOH and Na_2CO_3 series cannot be described by one common plot but by two independent curves.

4. DISCUSSION

The discussion of the results concerning the performance of the silver catalysts cannot be separated from extensive knowledge about the structure and mechanism of the copper catalysts' operation, as these two catalytic systems act similarly. The main controversy regarding the methanol catalysts is related to the existence of a synergy effect between Cu and oxide components (ZnO, ZrO_2) of the catalysts The ICI[55] and Campbell[56] groups claim that the synergy effect is not present in the copper catalysts, and that the hydrogenation of CO_2 to methanol and the RWGS reaction both occur on the surface of metallic copper. The support is only responsible for a high dispersion of copper. However, many authors provided extensive evidence[38] that the methanol formation rate expressed per one Cu site is one to two orders higher for the Cu/ZnO and Cu/ZnO/Al_2O_3 catalysts than for pure copper or for systems where copper is dispersed on specially purified SiO_2. The above studies clearly point to the existence of the synergy effect in the copper catalysts.

The results presented by Yoshihara and Campbell,[56] comparing the activities of Cu(110), polycrystalline copper, and Cu/ZnO in the CO_2 hydrogenation, are unconvincing as far as the synergy effect is concerned. They show that metallic copper is very active in the RWGS reaction, but the methanol formation rate is about two orders lower in comparison with the RWGS reaction. This stands in clear contradiction to the catalytic performance of the Cu/ZnO or Cu/ZnO/Al_2O_3 catalysts, which produce methanol with nearly 100% selectivity. It is fairly well-

dx.doi.org/10.1021/cs100033v |ACS Catal. 2011, 1, 266–278

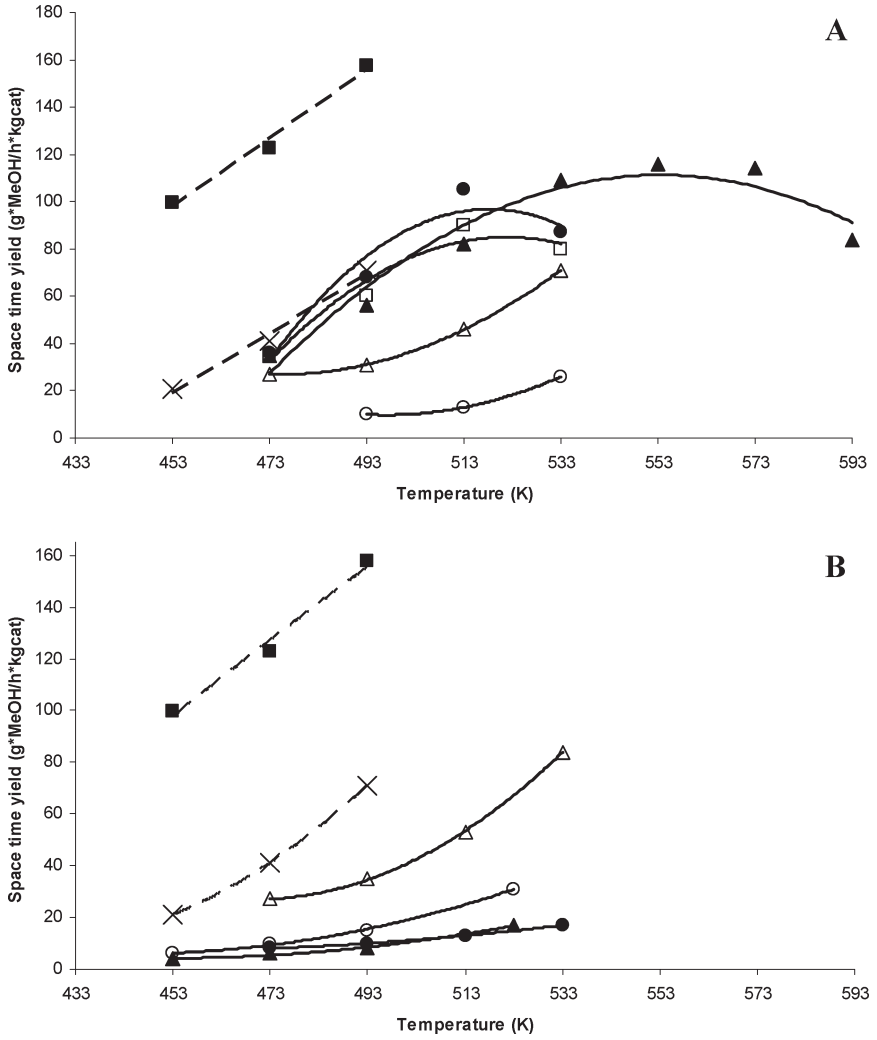

Figure 7. Catalytic activity of the silver catalysts in the methanol synthesis. (A) Obtained by the NaOH method; (B) obtained by the Na_2CO_3 method. Keys: Δ, ZrZnAg30; ○, ZnAg10; □, ZrAg30; ▲, ZrAg10; ●, ZrZnAg10; *, ZrZnAg62.5. Dashed line: ■, ZrZnCu 62.5; ×, ZrZnCu10 (according to ref 27).

known that one of the synergy aspects is stabilization of Cu^+, which favors the CO_2 hydrogenation to methanol. Cu^+ ions can be stabilized on the surface of ZnO,[31,32,35,36] ZrO_2,[24,33,34] and on the ZnO/ZrO_2 mixed systems as well.[29,30] Recently, an influence of different polymorphic forms of ZrO_2 (tetragonal or monoclinic) on the performance of Cu/ZnO or $Cu/ZnO/Al_2O_3$ has drawn more attention.[28,57]

The XRD investigations presented in our paper show that ZrO_2 is mainly present in a pseudomorphic form in the oxide precursors whereas it crystallizes as monoclinic and tetragonal phases in the used catalysts. Moreover, contents of these phases depend on the preparation method. The use of NaOH (pH = 10) clearly favors the formation of the tetragonal phase (t-ZrO_2) while the use of Na_2CO_3 (pH = 7) leads to catalysts in which the monoclinic (m-ZrO_2) phase predominates. These results are in agreement with reports of Baiker et al.[23] and Rhodes and Bell et al.[28]

It is believed that the stabilization of the t-ZrO_2 phase, which is thermodynamically unstable at low temperatures, is connected to formation of oxygen vacancies in the ZrO_2 structure or/and with the presence of alkali additives (Ca^{2+}, K^+, etc.).[58−61] The other factors that influence the t-ZrO_2 stabilization can be the surface hydroxylation (hydration) and high dispersion of ZrO_2 crystallites.

The TPR results presented in this paper show that ZrO_2, which is the component of the catalysts, is slightly reduced during the reaction, which is equivalent to the formation of oxygen vacancies. The same effect, observed in the used catalysts, is evidenced by a decrease of the ZrO_2 lattice parameters and by the fact that the used catalysts do not undergo reduction in the TPR experiments. The reduction degree of ZrO_2, estimated on the basis of the TPR results, is approximately 0.5% in relation to the total oxygen content in ZrO_2. Because oxygen mobility is negligible at the catalytic reaction temperature (Tamman temperature is around 2000 K), one should expect that concentration of oxygen vacancies in the surface layer would be considerably higher (for example 5% for a zone, which encompasses 10 atomic layers). The condition of electroneutrality can be fulfilled either by localization of the electrons on zirconium ions with the formation of Zr^{2+} ions or by the presence of additional positive ions in interstitial or lattice positions in the vicinity of the vacancies. It is obvious that these two processes can occur simultaneously.

The XPS and Auger measurements suggest that a small amount of Zr^{2+} or Zr^{4+} bonded to oxygen vacancies (that both

dx.doi.org/10.1021/cs100033v |*ACS Catal.* 2011, 1, 266–278

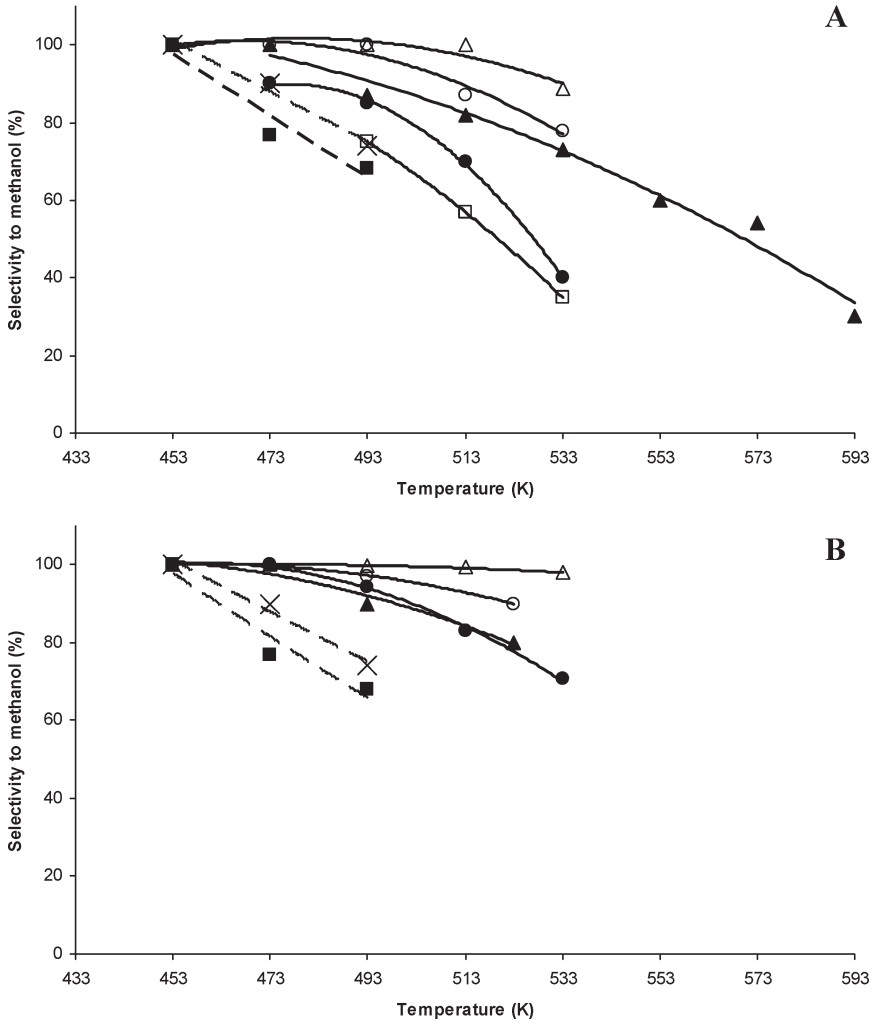

Figure 8. Selectivity to methanol of the silver catalysts. (A) Obtained by the NaOH method; (B) obtained by the Na_2CO_3 method; Keys: Δ, ZrZnAg30; ○, ZnAg10; □, ZrAg30; ▲, ZrAg10; ●, ZrZnAg10; *, ZrZnAg62,5. Dashed line: ■, ZrZnCu 62.5; ×, ZrZnCu10 (according to ref 27).

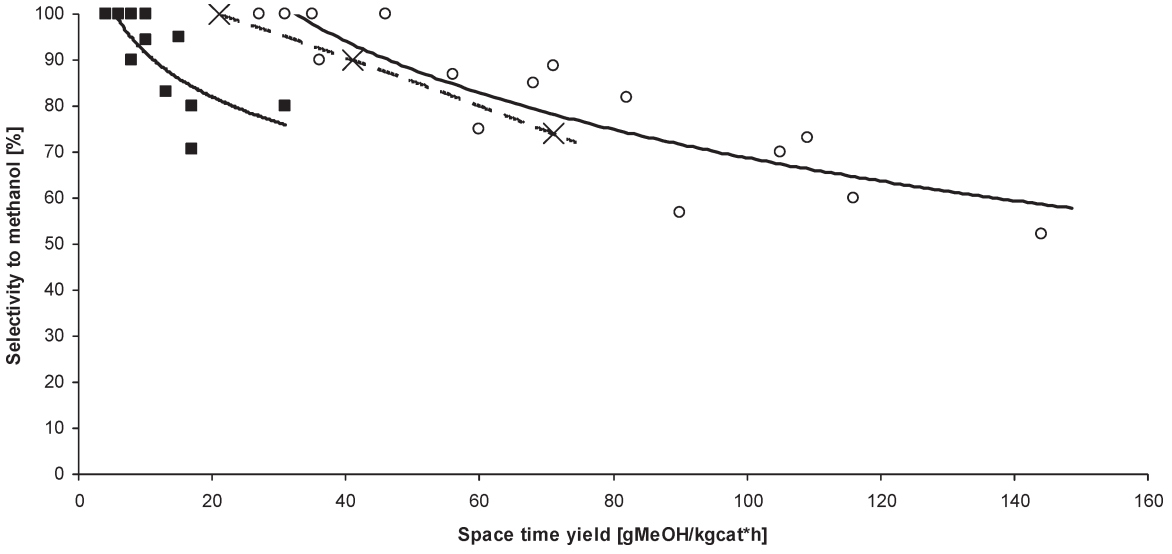

Figure 9. Selectivity to methanol versus space time yield of methanol for silver catalysts prepared by the NaOH (○) and Na_2CO_3 (■) methods. Keys: dashed line, ×. ZrZnCu10 (according to ref 27).

dx.doi.org/10.1021/cs100033v |*ACS Catal.* 2011, 1, 266–278

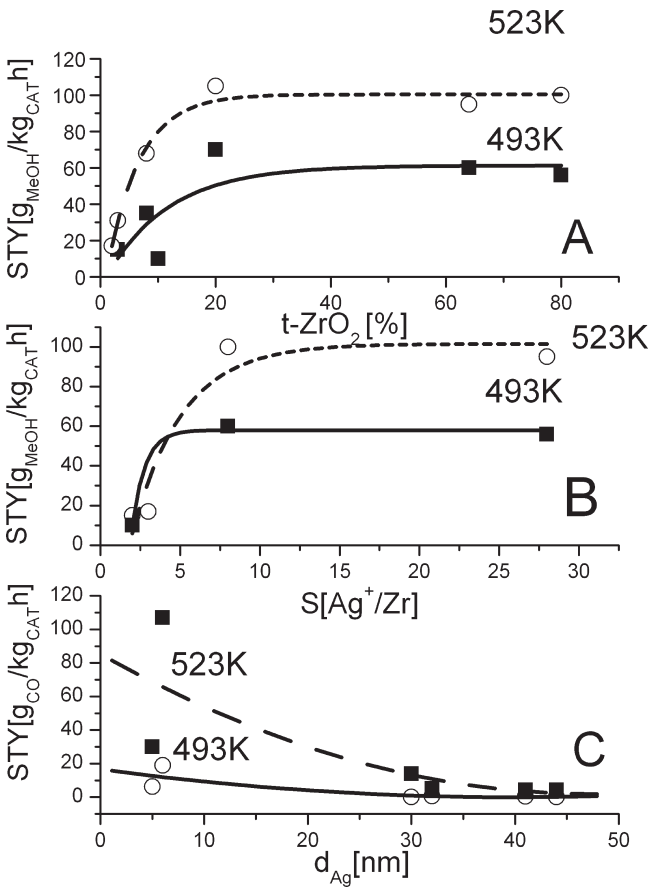

Figure 10. (A) Space time yield of methanol versus content of the t-ZrO_2 phase at 523 and 493 K for the silver catalysts obtained by the NaOH and Na_2CO_3 methods. (B) Space time yield of methanol versus content of surface Ag^+ per 1 g of catalyst at 523 and 493 K for the silver catalysts obtained by the NaOH and Na_2CO_3 methods. (C) Space time yield of CO versus mean dimension of silver crystals at 523 and 493 K for the silver catalysts obtained by the NaOH and Na_2CO_3 methods.

result in similar electronic state of zirconium) are present in the surface layer. These zirconium species together with substantial amount of Ag^+ ions can stabilize the t-ZrO_2 phase. The peak positions of Ag 3d and Ag MVV and their shapes hint that Ag^+ ions are in a strongly electronegative environment that is generated either by nonionized oxygen vacancies or by Zr^{2+} ions. Concluding, the stabilization of the t-ZrO_2 phase in the studied catalysts is connected to the presence of oxygen vacancies and Ag^+ ions, which are stable in the conditions of the catalytic reaction.

While describing the catalytic performance of silver catalysts, it must be stressed that no correlation between the catalyst activity in the methanol synthesis and the dispersion of metallic silver (Ag^0) was found. Moreover, both the activity and the selectivity practically do not depend on the total silver content. This observation reveals that the formation of methanol does not occur on the metallic silver surface but is determined by other factors.

The correlation between the catalytic activity (space time yield (STY) of methanol) and the content of t-ZrO_2 phase in the catalysts for both series of the catalysts (NaOH, Na_2CO_3) is presented in Figure 10A. In Figure 10B the STY dependence of methanol as a function of the Ag^+ is shown. The Ag^+/Zr ratio determined by XPS measurements (Table 5) was used for the determination of Ag^+ concentration in the surface layer. The product of this value and the specific surface area is the measure of the number of surface Ag^+ in a unit mass of catalyst. As observed from Figure 10 panels A and B the rate of methanol formation increases with an increase of the t-ZrO_2 phase and Ag^+ content These correlations can be explained assuming that methanol is formed on Ag^+ sites, which are stabilized by oxygen vacancies in the t-ZrO_2 phase. Thus nonstoichiometric t-ZrO_2 containing oxygen vacancies and Ag^+ stabilized on the surface is the active phase. A similar relationship is observed for the copper catalysts; it is postulated that Cu^+ ions facilitate CO_2 adsorption and thus the formation of the surface formate complexes that are consecutively hydrogenated to methanol.[34−37]

The rate of the parallel RWGS reaction, leading to the formation of CO and H_2O, increases with the metallic silver dispersion (Figure 10C). This reaction occurs on the surface of metallic silver by the surface species reaction (H, O, CO) being the products of H_2 and CO_2 dissociation in accordance with a simple redox mechanism, similarly as it was found for metallic copper and the Cu/ZnO catalysts.[37−41] On the basis of above correlations and by analogy to the copper catalysts, for the silver catalysts, the following catalytic network scheme can be proposed.

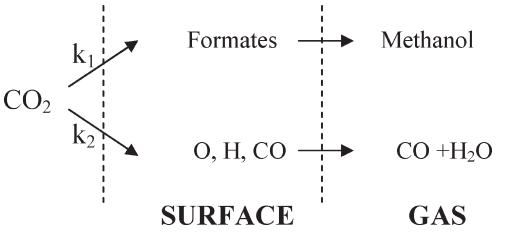

where rate constant k_1 is proportional to the Ag^+ content and therefore also to the content of the t-ZrO_2 phase and k_2 is proportional to the dispersion degree of metallic silver.

Finally, it is worth noticing a distinct difference between the copper and the silver catalysts. For the silver catalysts, the presence of ZnO in the support does not have any significant influence on the methanol formation rate. Thus, silver activation connected to the stabilization of Ag^+ occurs exclusively with the participation of the t-ZrO_2 phase. In the copper containing catalysts, the stabilization of Cu^+ ions can occur both on the surface of ZrO_2 and on ZnO.

The results described above can be confronted with limited literature information. Baiker et al.[23] showed that the catalysts containing Cu, Ag, or Au supported on t-ZrO_2 are highly active in the CO_2 hydrogenation to methanol, which is in agreement with the results presented in our paper while Jung and Bell[57] and Rhodes and Bell[28] who studied Cu/ZrO_2 catalysts containing pure phases of m-ZrO_2 or t-ZrO_2 obtained opposite results. The discrepancies can be explained by different concentration of oxygen vacancies in ZrO_2. The catalysts studied in refs 28,57 were obtained by impregnation, followed by calcinations at relatively low temperature and hydrogen treatment at low partial pressure. The catalysts studied in this work were prepared by coprecipitation and calcined at higher temperature. Furthermore, the catalysts were kept at temperatures above 500 K for a long period of time and in the reagent flow of high hydrogen partial pressure until the stationary state was reached. Under such conditions, oxygen vacancies and Ag^+ ions coupled with them

were observed in the ZrO_2 sublayer. Neither preparation conditions nor catalyst treatment used in refs 28 and 57 did favor formation of such defects.

■ ASSOCIATED CONTENT

Supporting Information. Further details are given in Figures S1−S18. This material is available free of charge via the Internet at http://pubs.acs.org.

■ AUTHOR INFORMATION

Corresponding Author
*E-mail: ncgrabow@cyf-kr.edu.pl.

■ ACKNOWLEDGMENT

The authors are grateful to Dr. Piotr Olszewski for his support in the synthesis of selected catalysts, to Dr. Małgorzata Ruggiero-Mikołajczyk and Dr. Małgorzata Zimowska for the BET and SEM measurements, respectively.

■ REFERENCES

(1) Halmann, M.L. . Process Sciences Group: Upton, NY, 1998; ISBN 10:1566702844.
(2) Haggin, J. *Chem. Eng. News* **1994**, *72*, 28–36.
(3) Hirano, M.; Akano, T.; Imai, T.; Kuroda, K. *Stud. Surf. Sci. Catal.* **1998**, *114*, 545–549.
(4) Breen, J. P.; Ross, J. R. H. *Catal. Today* **1999**, *51*, 521–533.
(5) Velu, S.; Suzuki, K.; Okazaki, M.; Kapoor, M. P.; Osaki, T.; Ohashi, F. *J. Catal.* **2000**, *194*, 373–384.
(6) de Wild, P. J.; Verhaak, M. J. F. M. *Catal. Today* **2000**, *60*, 3–10.
(7) Amenomiya, Y. *Appl. Catal.* **1987**, *30*, 57–68.
(8) Bartley, G. J. J.; Burch, R. *Appl. Catal.* **1988**, *43*, 141–153.
(9) Gasser, D.; Baiker, A. *Appl. Catal.* **1989**, *48*, 279–294.
(10) Köppel, R. A.; Baiker, A.; Wokaum, A. *Appl. Catal., A* **1992**, *84*, 77–102.
(11) Nitta, Y.; Fujimatsu, T.; Okamoto, Y.; Imanaka, T. *Catal. Lett.* **1993**, *17*, 157–165.
(12) Fröhlich, C.; Köppel, R. A.; Baiker, A. *Appl. Catal., A* **1993**, *106*, 275–293.
(13) Nitta, Y.; Suwata, O.; Ikeda, Y.; Okamoto, Y.; Imanaka, T. *Catal. Lett.* **1994**, *26*, 345–354.
(14) Sahibzada, M.; Chadwig, D.; Metcalfe, I. S. *Catal. Today* **1996**, *29*, 367–372.
(15) Kilo, M.; Weigel, J.; Baiker, A.; Wokaun, A.; Köppel, R. A.; Stoekli, A.; Baiker, A. *J. Mol. Catal. A: Chem.* **1997**, *126*, 169–184.
(16) Ma, Y.; Sun, Q.; Wu, D.; Fan, W.-H.; Zhan, Y.-L.; Deng, J.-F. *Appl. Catal., A* **1998**, *171*, 45–55.
(17) Joo, O.-S.; Jung, K.-D.; Moon, I.; Rozovskii, A. Ya.; Lin, G. I.; Han, S.-H.; Uhm, S.-J. *Ind. Eng. Chem. Res.* **1999**, *38*, 1808–1812.
(18) Wambach, J.; Baiker, A.; Wokaun, A. *Phys. Chem. Chem. Phys.* **1999**, *1*, 5071–5080.
(19) Ortelli, E. E.; Wambach, J.; Wokaun, A. *Appl. Catal., A* **2001**, *216*, 227–241.
(20) Chinchen, G. C.; Denny, P. J.; Jennings, J. R.; Spencer, M. S.; Waugh, K. C. *Appl. Catal.* **1988**, *36*, 1–65 (a review and references therein).
(21) Saito, M.; Fujitani, T.; Takeuchi, M.; Watanabe, T. *Appl. Catal., A* **1996**, *138*, 311–318.
(22) Słoczyński, J.; Grabowski, R.; Olszewski, P.; Kozłowska, A.; Stoch, J.; Lachowska, M.; Skrzypek, J. *Appl. Catal., A* **2006**, *310*, 127–137.
(23) Baiker, A.; Kilo, M.; Maciejewski, M.; Manzi, S.; Wokaun, A. *Stud. Surf. Sci. Catal.* **1993**, *75*, 1257–1272.
(24) Fröhlich, C.; Kapel, R. A.; Baiker, A.; Kilo, M.; Wokaun, A. *Appl. Catal., A* **1993**, *106*, 275–293.
(25) Köppel, R. A.; Stöcker, C.; Baiker, A. *J. Catal.* **1998**, *179*, 515–527.
(26) Köppel, R. A.; Baiker, A.; Schied, Ch.; Wokaun, A. *J. Chem. Soc., Faraday Trans* **1991**, *87*, 2821–2828.
(27) Słoczyński, J.; Grabowski, R.; Kozłowska, A.; Olszewski, P.; Stoch, J.; Skrzypek, J.; Lachowska, M. *Appl. Catal.* **2004**, *278*, 11–23.
(28) Rhodes, M. D.; Bell, A. T. *J. Catal.* **2005**, *233*, 198–209.
(29) Saito, M.; Fujitani, T.; Takahara, I.; Watanabe, T.; Takeuchi, M.; Kanai, Y.; Moriya, K.; Kakumoto, T. *Energy Convers. Manage.* **1995**, *36*, 577–580.
(30) Saito, M.; Fujitani, T.; Takeuchi, M.; Watanabe, T. *Appl. Catal., A* **1996**, *138*, 311–313.
(31) Klier, K. *Adv. Catal.* **1982**, *31*, 243–318.
(32) Okamoto, Y.; Fukino, K.; Imanaka, T.; Teraniski, S. *J. Phys. Chem.* **1983**, *87*, 3747–3754.
(33) Liu, J.; Shi, J.; He, D.; Zhang, Q.; Wu, X.; Liang, Yu.; Zhu, Q. *Appl. Catal., A* **2001**, *218*, 113–119.
(34) Suh, Y. W.; Moon, S.-H.; Rhee, H.-K. *Catal. Today* **2000**, *63*, 447–452.
(35) Toyir, J.; de la Piscina, P. R.; Fierro, J. L. G.; Homs, N. *Appl. Catal., B* **2001**, *29*, 207–215.
(36) Toyir, J.; de la Piscina, P. R.; Fierro, J. L. G.; Homs, N. *Appl. Catal., B* **2001**, *34*, 255–266.
(37) Hansen, J. B. *Handbook of Heterogenous Catalysis*; VCH-Wiley: Weinheim, Germany, 1997; Vol. 4, pp 1856−1876 (and references therein).
(38) Skrzypek, J.; J. Słoczyński, Ledakowicz, S. *Metanol Synthesis*; Polish Scientific Publishers (PWN): Warszawa, Poland, 1994; ISBN 83-01-11490-9.
(39) Salmi, T.; Hakkarainen, R. *Appl. Catal.* **1989**, *49*, 285–306.
(40) Nakamura, J.; Campbell, J. M.; Campbell, Ch.T. *J. Chem. Soc., Faraday Trans.* **1990**, *86*, 2725–2734.
(41) Ernst, K. H.; Campbell, Ch.T.; Moretti, G. *J. Catal.* **1992**, *134*, 66–74.
(42) Nitta, Y.; Suwata, O.; Ikeda, Y.; Okamoto, Y.; Imanaka, T. *Catal. Lett.* **1994**, *26*, 345–354.
(43) Cheary, R. W.; Coelho, A. A. *J. Appl. Crystallogr.* **1992**, *25*, 109–121.
(44) *Powder Diffraction File*; International Centre of Diffraction Data (ICCD) : Newtown Square, PA, 2009.
(45) Dow, W.-P.; Wang, Y.-P.; Huang, T.-J. *J. Catal.* **1996**, *160*, 155–170.
(46) Tanuma, S.; Powell, C. J.; Penn, D. R. *Surf. Interface Anal.* **1993**, *21*, 165.
(47) Moulder, J. F.; Stickle, W. F.; Sobol, P. E.; Bomben, K. *Handbook of X-ray Photoelectron Spectroscopy*, 2nd ed.; Chastain, J., Ed.; Perkin-Elmer Corporation (Physical Electronics): Eden Prairie, MN, 1992.
(48) *NIST X-ray Photoelectron Spectroscopy Database*; National Institute of Standards and Technology: Gaithersburg, MD; http://srdata.nist.gov/xps/
(49) Wang, L.-C.; Liu, Q.; Chen, M.; Liu, Y.-M.; Cao, Y.; He, H.-Y.; Fan, K.-N. *J. Phys. Chem. C* **2007**, *111*, 16549–16557.
(50) Kumar, L.; Sarma, D. D.; Krummacher, S. *Appl. Surf. Sci.* **1988**, *32*, 309.
(51) Zemlyanov, D. Y.; Nagy, A.; Schlogl, R. *Appl. Surf. Sci.* **1998**, *133*, 171–183(J.A. 8).
(52) Kibis, L. S.; Avdeev, V. I.; Koscheev, S. V.; Boronin, A. I. *Surf. Sci.* **2010**, *604*, 1185–1192.
(53) Rodriguez, J. H. *J. Phys. Chem.* **1994**, *98*, 4061–406.
(54) Bera, S.; Gangopadhyay, P.; Nair, K. G. M.; Panigrahi, B. K.; Narasimhan, S. V. *J. Electron Spectrosc. Relat. Phenom.* **2006**, *152*, 91–95.
(55) Bailey, S.; Froment, G. F.; Snoeck, J. W.; Waugh, K. C. *Catal. Lett.* **1995**, *30*, 99–111.
(56) Yoshihara, J.; Campbell, Ch.T. *J. Catal.* **1996**, *161*, 776–782.
(57) Jung, K. T.; Bell, A. T. *Catal. Lett.* **2002**, *80*, 63–68.

(58) Stefanovich, E. V.; Shluger, A. L. *Phys. Rev. B* **1994**, *49*, 11560–11571.
(59) Bechepeche, A. P.; Treu, O.; Longo, J. E.; Paiva-Santos, C. O.; Varela, J. A. *J. Mater. Sci.* **1999**, *34*, 2751–2756.
(60) Hleis, D.; Labaki, M.; Laversin, H.; Courcot, D.; Aboukais, A. *Colloids Surf., A* **2008**, 193–200.
(61) Li, P.; Chen, I.-W.; Penner-Hahn, J. E. *J. Am. Ceram. Soc.* **1994**, *77* (5), 1281–1288.